Performance Study for Jet Energy Resolution of the Dual-Readout Calorimeter

Kyuyeong Hwang[1,*] on behalf of Korean Dual-Readout Calorimeter R&D Collaboration

[1]Department of Physics, Yonsei University, Seoul, 03722, Korea

Abstract. In calorimetry, the imperfect hadronic energy resolution of non-compensating calorimeters is caused mainly by the non-Gaussian fluctuation of the electromagnetic fraction and that in binding energy loss. To address this problem, the Dual-readout method was proposed and validated through beam tests over the last 20 years. This study investigates the jet energy resolution achieved using GEANT4 simulations. Key result highlights an improved jet energy resolution of 3.66% for 100 GeV jets, satisfying the requirements of future e^+e^- collider experiments.

1 Introduction

The Dual-readout calorimeter (DRC) leverages two independent signals from scintillation and Čerenkov photons to measure the electromagnetic fraction of hadronic showers and compensate hadronic energies on an event-by-event basis. Over two decades, the DRC's performance has been validated through beam tests and simulations [1], making it a candidate for inclusion in future e^+e^- collider experiments such as FCC-ee [3] and CEPC [8]. This paper presents a performance study of the DRC using GEANT4 simulations [2], focusing on its capability to achieve high-precision energy measurements for electromagnetic, hadronic, and jet particles.

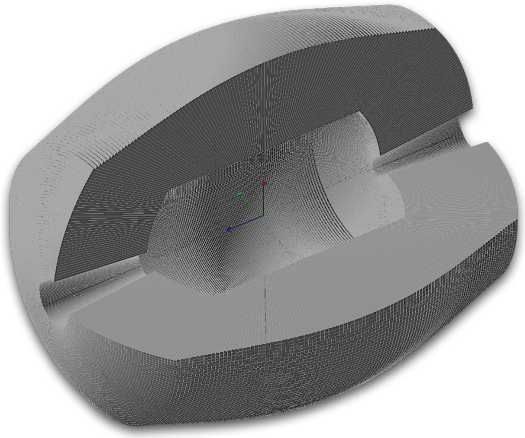

Figure 1. Calorimeter implemented in GEANT4 simulation.

2 Simulation setup

The structure of the calorimeter is optimized with respect to absorber material, ratio of active material to absorber material, space between optical fibers, etc.

The DRC covers a near 4π solid angle as shown in figure 1. It is composed of about 52,000 individual towers, each tower is composed of a copper absorber and 1 *mm* radius optical fiber spaced by 0.5 *mm*. Towers have a 2.5 *m* depth, corresponding to 10 nuclear interaction length (λ_{int}), allowing us to catch 99% of the energy deposit.

Two types of fibers are implemented: scintillation and Čerenkov ones. For the scintillation fiber, we choose Kuraray SCSF-78 which is made of polymethylmethacrylate (PMMA) cladding and polystyrene based scintillating core. For the Čerenkov fiber, we choose Mitsubishi ESKA SK-40 which is composed of fluorinated polymer cladding and PMMA core. Optical physics properties of each material, such as material composition and refractive index, are based on manufacturer specifications. At the end of each fiber, a silicon photomultiplier (SiPM) is attached, composing a high-granularity readout array. We implement the detection efficiency of SiPM as the Hamamatsu S13615-1025 sensor to consider the counting of detected photoelectron during the simulation.

Magnetic field is not applied for the simulations to evaluate the intrinsic performance of the calorimeter. With the magnetic field, some shower particles cannot reach the detector, leading to a slight reduction in detection resolution that is beyond the scope of this study.

We conduct the simulations with full optical propagation with GEANT4 version 10.5.p01. Full optical simulation takes more time and resources than other simulations, but it is expected to obtain the more realistic results. Through this simulation study, we expect more reasonable and accurate results in DRC performance for future e^+e^- colliders.

*e-mail: khwang@cern.ch

3 Analysis procedure

3.1 Calibration

Calibration is performed using a 20 GeV electron beam directed at the center of the towers with 1 cm^2 square shaped beam spot. To avoid the discrepancy in responses with respect to the impact point of incident beam particles, the beam is inclined by 1.5° with the tower axis.

$$Q^2 = \sum_j \left[\sum_i C^i {N_{pe}}^{ij} - 20GeV \right]^2 \quad (1)$$

The calibration constants (C^i) were determined by minimizing the chi-squared function defined in equation 1, which is the residual of measured energy and incident particle energy, using the minimum gradient method. i and j stand respectively for the indices of the tower and the simulated event. ${N_{pe}}^{ij}$ is the number of photoelectrons detected on i th tower from j th event. The result of calibration constants is shown in figure 2.

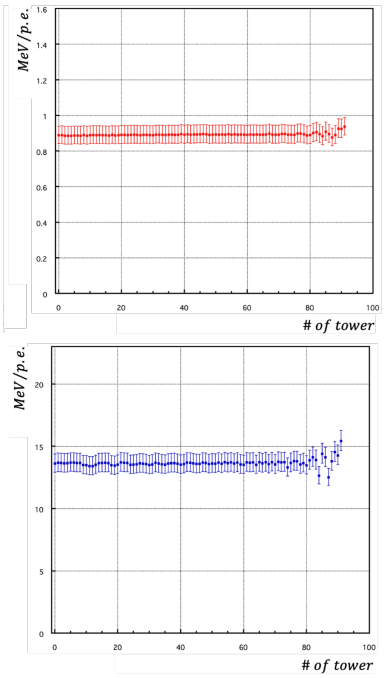

Figure 2. Calibration constants of scintillation channel (top) and Čerenkov channel (bottom).

With the result of calibration constants, we can estimate the energy of each simulation, as shown in Figure 3. As the left side of figure 3 shows good agreement between scintillation channel (red) and Čerenkov channel (blue) to 20 GeV, we can assure that the calibration constants are well estimated for electrons.

3.2 EM energy resolution

With the calibration constants introduced in Sect. 3.1, we can measure the energy and its resolution of each channel. The electromagnetic energy resolution is estimated with e^- simulations with energies ranging from 5 GeV to 110 GeV. The e^- beam has an inclination of 1.5°, a span of 1 cm^2 beam spot and aims at the center of the tower located on xy plane[1].

The left side of figure 4 shows the linear relationship between beam energy and measured energy for both fiber types and their sum. It shows a linearity within 1%. The right side of figure 4 shows the resolution, after linearity.

$$\frac{\sigma}{E} = \frac{stochastic\ term}{\sqrt{E}} + constant\ term \quad (2)$$

As we can parameterize the resolution with two parameters in equation 2, stochastic and constant term, we estimate both constants of each channel. Scintillation and Čerenkov channels are independent of each other, we can simply add their responses event-by-event to get much better resolution as denoted with "Summed" in figure 4.

With the single e^- simulation, we estimate the EM energy resolution of the DRC with 11.5% for the stochastic term and 0.2% for the constant term.

3.3 Hadronic energy resolution

Hadronic energy resolution of the DRC is estimated with single pi^+ simulations with energies ranging from 5 GeV to 110 GeV with same inclination, direction and beam spot size applied to e^- simulation in Sect. 3.2. We introduce the dual-readout method to this simulation to adjust imperfect energy measurement of hadronic shower. For the dual-readout method, we applied 0.291 for correction factor, which measured via test beam experiments [1].

As shown on the left side of figure 5, dual-readout corrected energy shows improved linearity compared to scintillation and Čerenkov channels. Resolution of hadronic particles is estimated to be 22.4% for the stochastic term and 0.9% for the constant term, as shown on the right side of figure 5.

Hadronic energy resolution for conventional calorimeter is 7% for ATLAS and 12% for CMS [5] with 100 GeV hadron. The DRC shows improved hadronic energy resolution with 3.14% for 100 GeV pi^+.

3.4 Jet energy resolution

To estimate jet energy resolution, We generate u quark and $\bar{u}$ quark events, without initial radiation to ensure back-to-back jet orientation. Event generation and hadronization of quarks are done with Pythia8 [4].

Bottom side of figure 3 shows the measured energy distribution for 40 GeV of u and $\bar{u}$ jets, for a total event energy of 80 GeV. Thus, DR corrected energy shows its mean value as 79.1 GeV near 80 GeV.

Figure 6 shows the linearity and resolution results. Linearity is recovered after applying dual-readout correction. Also, resolution for the dual-readout corrected energy shows the improved resolution compared to scintillation and Čerenkov channels. The jet energy resolution is

[1]Origin is located at the center of the calorimeter and Z axis defined as beam line.

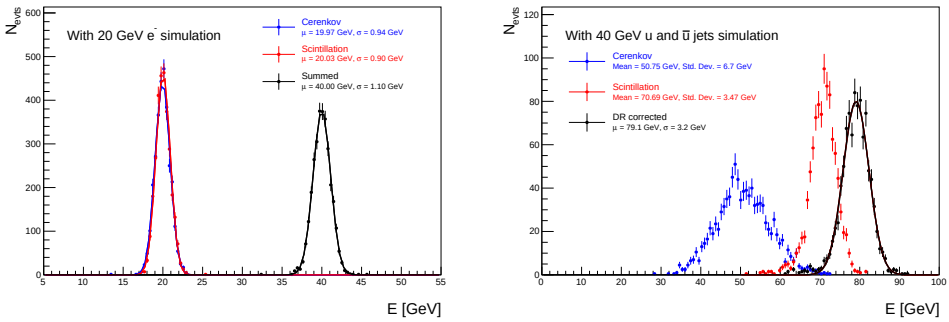

Figure 3. Measured energy with 20 GeV electron (left), and 40 GeV u and $\bar{u}$ jets (right) simulations. For jets simulations, $\chi = 0.291$ is used.

estimated to have a stochastic term of 34.6% and a constant term of 0.2%

Result of jet energy resolution with a pure calorimetric measurement accomplishes 3.66% resolution for 100 GeV jet, while the CMS and ATLAS shows 12% and 10% of jet energy resolution for 100 GeV p^T jet [6, 7]. The DRC meets the requirements for the calorimeter of future e^+e^- collider experiments.

3.5 Mass separation

The most important aspect of the calorimeter for the future e^+e^- collider is invariant mass separation of hadronically decaying bosons. We validate the invariant mass separation between bosons using jet events explained in Sect. 3.4.

Figure 7 shows energy separation between 80 GeV, 91 GeV and 125 GeV jet events which are corresponding to W, Z and H invariant mass. The energy distributions are well separated from each other, which proves that the DRC can achieve the invariant mass separation of bosons.

4 Summary

As a novel technology which has been researched for the last 20 years, the DRC has sufficient performances and properties requested as a calorimeter of the future e^+e^- collider experiments such as FCC-ee and CEPC. We design the optimized calorimeter structure based on previous study and implement the properties of each part with the products that we can utilize for production.

We conducted full optical simulation in GEANT4, expecting the more reasonable and accurate result for estimating the performance of the DRC. Calibration is performed with 20 GeV e^- simulations. The stochastic term of energy resolution is estimated to be 11.5% for electromagnetic particles, 22.4% for hadronic particles.

Jet events are generated with Pythia8 composing with u and $\bar{u}$ quarks having same energy and back-to-back momentum direction. With simulation through generated events, the stochastic term of jet energy resolution is estimated to be 34.6%, which satisfies the requirement for calorimeter of the future e^+e^- collider.

The most important aspect of the calorimeter for the future e^+e^- colliders is the invariant mass separation between hadronically decaying bosons. With the generated jet events used for energy resolution estimation are utilized to validate it. The DRC shows reasonable energy separation among jet events which are corresponding to boson's invariant mass.

References

[1] S. Lee, M. Livan, R. Wigmans, Dual-readout calorimetry. Reviews of Modern Physics **90**, 025002 (2018). https://doi.org/10.1103/RevModPhys.90.025002

[2] S. Agostinelli, *et al*, Geant4—a simulation toolkit. Nuclear Instruments and Methods in Physics Research Section A: Accelerators, Spectrometers, Detectors and Associated Equipment **506**, 250 (2003). https://doi.org/10.1016/S0168-9002(03)01368-8

[3] A. Abada, *et al*, FCC-ee: The Lepton Collider : Future Circular Collider Conceptual Design Report Volume 2. European Physics Journal Special Topics **228**, 261 (2019). https://doi.org/10.1140/epjst/e2019-900045-4

[4] T. Sjöstrand, *et al*, An introduction to PYTHIA 8.2. Computer Physics Communications **191**, 159 (2015). https://doi.org/10.1016/j.cpc.2015.01.024

[5] C. Lippmann, Particle identification. Nuclear Instruments and Methods in Physics Research Section A: Accelerators, Spectrometers, Detectors and Associated Equipment **666**, 148 (2012). https://doi.org/10.1016/j.nima.2011.03.009

[6] G. Agarwal, Jet Energy Scale and Resolution Measurements in CMS, Proceedings of 41st International Conference on High Energy physics — PoS(ICHEP2022) **414**, 652 (2022). https://doi.org/10.22323/1.414.0652

[7] The ATLAS Collaboration, Jet energy scale and resolution measured in proton–proton collisions at $\sqrt{s} = 13$ TeV with the ATLAS detector. The European Physical Journal C **81**, 689 (2021). https://doi.org/10.1140/epjc/s10052-021-09402-3

[8] The CEPC Study Group, CEPC Conceptual Design Report: Volume 2 - Physics Detector. https://doi.org/10.48550/arXiv.1811.10545

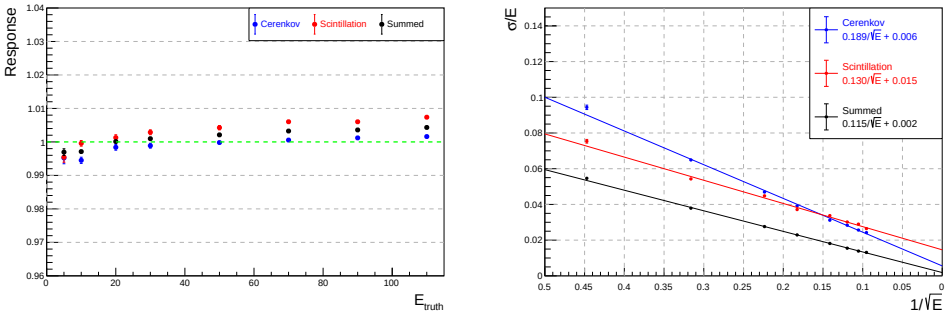

Figure 4. Linearity relationship between beam energy and measured energy (left) and resolution (right) with single e^- simulations

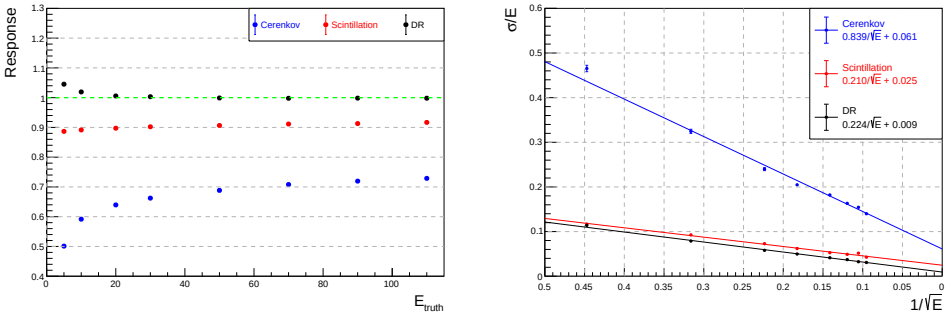

Figure 5. Linearity relationship between beam energy and measured energy (left) and resolution (right) with single pi^+ simulations

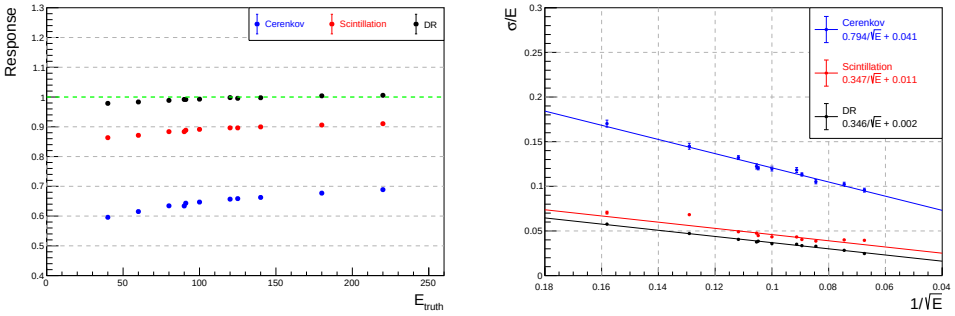

Figure 6. Linearity relationship between beam energy and measured energy (left) and resolution (right) with u and $\bar{u}$ jets simulations

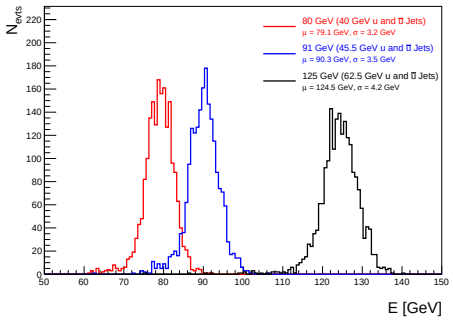

Figure 7. Energy separation between jet events which are corresponding to W (red), Z (blue) and H (black) bosons.